Supercontinuum generation in a water-core photonic crystal fiber

Alexandre Bozolan[1,*], Christiano J. S. de Matos[1], Cristiano M. B. Cordeiro[2], Eliane M. dos Santos[2] and John Travers[3]

[1]*Laboratório de Comunicações Ópticas e Fotônica – Univ. Presbiteriana Mackenzie – São Paulo – SP – Brazil*
[2]*Instituto de Física "Gleb Wataghin" – UNICAMP – Campinas – SP – Brazil*
[3]*Femtosecond Optics Group, Physics Department, Imperial College London - UK*
* - bozolan@sel.eesc.usp.br

Abstract: Supercontinuum generation is demonstrated in a 5-cm-long water-core photonic crystal fiber pumped near water's zero-dispersion wavelength. Up to 500-nm spectral width (evaluated at -20 dB from the peak) is achieved, while spectral widths were over 4 times narrower with a bulk setup at the same wavelength and peak power, and over 3 times narrower if the PCF was pumped away from the zero-dispersion wavelength. The supercontinuum generation mechanisms for bulk and waveguide setups are compared and tuning of the zero-dispersion wavelength via waveguide dispersion is theoretically investigated.

OCIS codes: (320.6629) Supercontinuum generation; (060.5295) Photonic crystal fibers; (010.7340) Water.

References and links

1. R. R. Alfano and S. L. Shapiro, "Observation of self-phase modulation and small-scale filaments in crystals and glasses," Phys. Rev. Lett. **24**, 592-596 (1970).
2. R. R. Alfano, *The supercontinuum laser source*, 2nd Edition (Springer-Verlag, New York, 1989).
3. C. Lin and R. H. Stolen, "New nanosecond continuum for excited-state spectroscopy," Appl. Phys. Lett. **28**, 216-218 (1976).
4. J. K. Ranka, R. S. Windeler, and A. J. Stentz, "Visible continuum generation in air-silica microstructure optical fibers with anomalous dipersion at 800 nm," Opt. Lett. **25**, 25-27 (2000).
5. J. M. Dudley, G. Genty, and S. Coen, "Supercontinuum generation in photonic crystal fiber," Rev. Mod. Phys. **78**, 1135-1184 (2006).
6. P. St. J. Russell, "Photonic-Crystal fibers," J. Lightwave Technol. **12**, 4729-4749 (2006).
7. G. Humbert, W. J. Wadsworth, S. G. Leon-Saval, J. C. Knight, T. A. Birks, P. St. J. Russell, M. J. Laderer, D. Kopf, K. Wiesauer, E. I. Breuer, and D. Stifter, "Supercontinuum generation system for optical coherence tomography based on tapered photonic crystal fibre," Opt. Express **14**, 1596-1603 (2006).
8. R. Holzwarth, J. Reichert, T. Udem, T. W. Hänsch, J. C. Knight, W. J. Wadsworth, and P. St. J. Russell "An optical frequency synthesizer for precision spectroscopy," Phys. Rev. Lett. **85**, 2264-2267 (2000).
9. J. Hult, R. S. Watt, and C. F. Kaminski, "Dispersion measurement in optical fibers using supercontinuum pulses," J. Lightwave Technol. **25**, 820-824 (2007).
10. S. V. Smirnov, J. D. Ania-Castanon, T. J. Ellingham, S. M. Kobtsev, S. Kukarin, and S. K. Turitsyn, "Optical spectral broadening and supercontinnum generation in telecom applications," Opt. Fiber Technol. **12**, 122-147 (2006).
11. J. M. Fini, "Microstructure fibres for optical sensing in gases and liquids," Meas. Sci. Technol. **15**, 1120-1128 (2004).
12. S. Smolka, M. Barth, and O. Benson, "Highly efficient fluorescence sensing with hollow core photonic crystal fibers," Opt. Express **15**, 12786-12891 (2007).
13. S. Yiou, P. Delaye, A. Rouvie, J. Chinaud, R. Frey, G. Roosen, P. Viale, S. Férvrier, P. Roy, J. L. Auguste, and J. M. Blondy, "Stimulated Raman scattering in an ethanol core microstructured optical fiber," Opt. Express **13**, 4786-4791 (2005).
14. R. Zhang, J. Teipel, and H. Giessen, "Theoretical design of a liquid-core photonic crystal fiber for supercontinuum generation," Opt. Express **14**, 6800-6812 (2006).
15. A. S. L. Gomes, E. L. Falcão-Filho, C. B. de Araújo, D. Ratativa, and R. E. de Araújo, "Thermally managed eclipse Z-scan," Opt. Express **15**, 1712-1717 (2007).
16. P. Dumais, C. L. Callender, J. P. Noad, and C. J. Ledderhof, "Integrated liquid core waveguides for nonlinear optics," Appl. Phys. Lett. **90**, 101101 (2007).

#95587 - $15.00 USD Received 29 Apr 2008; revised 7 Jun 2008; accepted 7 Jun 2008; published 16 Jun 2008

17. L. Xiao, W. Jin, M. S. Demokan, H. L. Ho, Y. L. Hoo, and C. Zhao, "Fabrication of selective injection microstructured optical fibers with a conventional fusion splicer," Opt. Express **13**, 9014-9022 (2005).
18. A. G. V. Engen, S. A. Diddams, and T. Clement, "Dispersion measurements of water with white-light interferometry," Appl. Opt. **37**, 5679-5686 (1998).
19. M. J. Weber, *Handbook of Optical Materials* (CRC Press, Boca Raton, 2002).
20. G. P. Agrawal, *Nonlinear Fiber Optics*, 3rd Edition (Academic Press, San Diego, 2001).
21. I. Santa, P. Foggi, R. Righini, and J. H. Williams, "Time-resolved optical Kerr effect measurements in aqueous ionic solutions," J. Phys. Chem. **98**, 7692-7701 (1994).
22. L. de Boni, A. A. Andrade, L. Misoguti, C. R. Mendonça, and S. C. Zilio, "Z-scan measurements using femtosecond continuum generation," Opt. Express **12**, 3921-43927 (2004).
23. A. Brodeur and S. L. Chin, "Ultrafast white-light continuum generation and self-focusing in transparent condensed media," J. Opt. Soc. Am. B **16**, 637-650 (1999).
24. A. L. Gaeta, "Catastrophic collapse of ultrashort pulses," Phys. Rev. Lett. **84**, 3582-3585 (2000).
25. M. Kolesik, G. Katona, J. V. Moloney, and E. M. Wright, "Physical factors limiting the spectral extent and band gap dependence of supercontinuum generation," Phys. Rev. Lett. **91**, 43905 (2003).
26. Crystal Fibre A/S, http://www.crystal-fibre.com.
27. Y.–F. Li, M. C.–Y. Wang, and M.–L. Hu, "A fully vectorial effective index method for photonic crystal fibers: application to dispersion calculation," Opt. Commun. **238**, 29-33 (2004).

1. Introduction

Ever since their first demonstration, photonic crystal fibers (PCFs) have been employed for a wide range of purposes, among which supercontinuum generation has so far proved to be one of the most successful. Supercontinuum generation has long been known and studied in bulk materials [1,2] (including water [2]) and in conventional fibers [3]. Nevertheless, a significant reduction in the required powers and/or pulse energies has been achieved with the use of solid-core PCFs [4,5]. In this case, the cladding microstructure can both confine light to wavelength-scale cores and substantially control chromatic dispersion [6]. The use of PCFs presenting small cores and zero dispersion near the pump wavelength has, thus, made supercontinuum sources available for a range of practical applications such as optical coherence tomography [7], frequency metrology [8] and telecommunications [9,10].

On the other hand, liquid-filled PCFs have been studied in the last few years because the efficient light-sample interaction within the microstructure enables applications in fields such as sensing, spectroscopy and nonlinear optics [11-13]. In particular, the insertion of liquids in PCFs introduces new degrees of freedom with which nonlinear effects can be observed and controlled. The insertion of ethanol into the core of a hollow-core PCF, for example, has led to the observation of two Raman Stokes orders of this liquid [13]. The possibility of obtaining supercontinuum generation in a PCF whose core is filled with highly nonlinear liquids (CS_2 and nitrobenzene) has been recently theoretically studied [14]. The high nonlinear refractive indices of these liquids (2.2×10^{-15} cm^2/W for CS_2 [15]) and near-zero-dispersion pumping, obtained via waveguide dispersion engineering, contributes to efficient spectral broadening. Experimental supercontinuum generation in a toluene-core silica-cladding integrated waveguide has also been demonstrated [16]. However, in this case operation occurred in the normal dispersion region and the high cladding index limited the choice of the liquid.

In this work, we experimentally demonstrate supercontinuum generation utilizing a PCF whose core was filled with distilled water through a selective hole filling process [17]. The choice of water, which presents a nonlinear refractive index (1.6×10^{-16} cm^2/W [15]) an order of magnitude lower than that of CS_2 is justified due to its widespread availability, ease of manipulation, low volatility (30× less volatile that CS_2 at room temperature), and, most importantly, due to the fact that it presents a zero-dispersion wavelength of ~1066 nm [18]. A wide range of Q-switched and mode-locked lasers operate at this wavelength, facilitating supercontinuum generation. On the other hand, water absorption steeply increases with wavelength in the near infrared and has to be taken into account.

Here, we compare the nonlinear spectral broadening obtained with two pump wavelengths: 800 nm and ~980 nm. While at the former water presents a lower attenuation coefficient (0.02 cm^{-1} against 0.51 cm^{-1} at ~980 nm [19]), at the latter water exhibits a lower

#95587 - $15.00 USD Received 29 Apr 2008; revised 7 Jun 2008; accepted 7 Jun 2008; published 16 Jun 2008

dispersion (-18 ps/(nm.km) against -71 ps/(nm.km) at 800 nm [18]). Results show the pump's proximity to the zero dispersion wavelength by far compensates for the increased loss at ~980 nm. In addition, we compare these results with supercontinuum generation in bulk water and show that the confinement provided by guidance both radically lowers the power required for nonlinear broadening and changes the supercontinuum formation dynamics.

2. Experimental setup

The experimental setup is shown in Fig. 1. 60-fs pulses with a repetition rate of 1 kHz from an optical parametric amplifier (OPA) were coupled into ~5 cm of a PCF, the hollow core of which was filled with distilled water. Light from the OPA first passed through a longpass filter, which removed undesired spectral components, and a variable neutral-density filter. The beam was subsequently focused onto the PCF with a 20× objective and collected at the output with a 40× objective. Prior to the experiment, the 40× objective was used to image the fiber output in a CCD camera to ensure that a large fraction of light propagated through the core and that the fundamental mode was predominantly excited. For this mode, the PCF waveguide dispersion is expected to be small compared with the material dispersion (see section 4). The camera was then replaced with a second 20× objective that coupled the beam into a multimode fiber connected to an optical spectrum analyzer (OSA). Measurements were made with the OPA operating both at 800 nm and 980 nm.

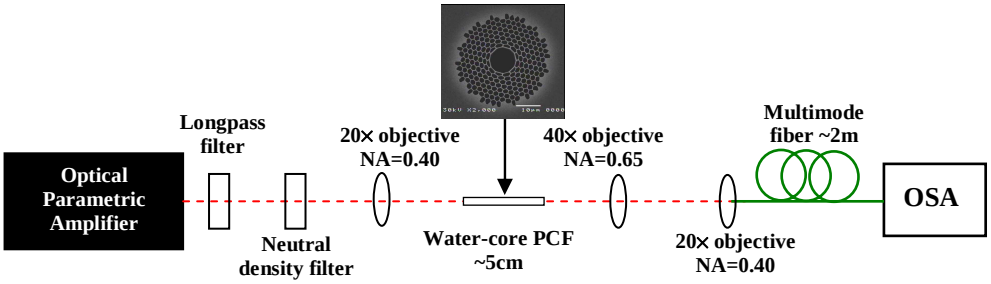

Fig. 1. Experimental setup used for obtaining supercontinuum generation in a water-core PCF and SEM image of the PCF's cross-sectional profile.

The cross section of the PCF used in the experiments is also shown in Fig. 1 and consists of a 10.7-μm-diameter core and a cladding microstructure with a pitch of ~2.2 μm and a hole diameter of ~1.9 μm. The high cladding air-filling fraction (~70%) means that the cladding effective index is sufficiently low to ensure light is guided through total internal reflection in the water core. The power coupled into the PCF was estimated by measuring the PCF output power, taking into account water's attenuation and neglecting all other possible loss sources. The estimated coupled peak (average) power was varied from 90 kW to 1.45 MW (~6 μW to ~92 μW) with the neutral-density filter. The spectral width of input pulses (measured at -20 dB from the peak) was ~65 nm.

A control experiment was undertaken with the water-filled PCF replaced with an air-core PCF. Light was then coupled into the thin glass layer between the core and the microstructured cladding and any spectral broadening analyzed. Although this case leads to propagation conditions that significantly differ from those of the water-core PCF, it may give an indication of the achievable spectral broadening induced by surface modes in the filled-PCF case. In addition, the water-core PCF results were compared with those of an equal setup but with the fiber replaced with a ~7-cm-long bulk cell filled with distilled water, and the input and output objectives replaced with 10-cm and 15-cm focal length lenses respectively.

3. Results and discussion

Figure 2 shows a comparison of the spectra obtained at 800 nm and 980 nm with the water-core PCF and three different coupled peak powers between 90 kW and 940 kW. Figure 2(a) shows the spectra for an 800-nm pump. It is apparent that only a moderate nonlinearity-driven

#95587 - $15.00 USD Received 29 Apr 2008; revised 7 Jun 2008; accepted 7 Jun 2008; published 16 Jun 2008

broadening takes place, with a maximum achieved width of 140 nm (at -20 dB from the peak). Figure 2(b) depicts the spectra obtained with a 980-nm pump. As the coupled power is increased, the spectrum significantly broadens, evolving into a supercontinuum. At a power of 940 kW a ~460-nm-wide spectrum (at -20 dB) is observed. In fact, the transmission spectrum over 5 cm of water [19] (also plotted in Fig. 2) indicates that the spectral expansion toward long wavelengths is stopped by the steep increase of water absorption near 1200 nm, limiting the obtained width. It is noted that the control experiment undertaken with the air-core PCF yielded a maximum spectral width of ~150 nm (with 980-nm pumping). In the water-core PCF experiment, the contribution of silica to spectral broadening is expected to be even smaller, as most light travels through the core.

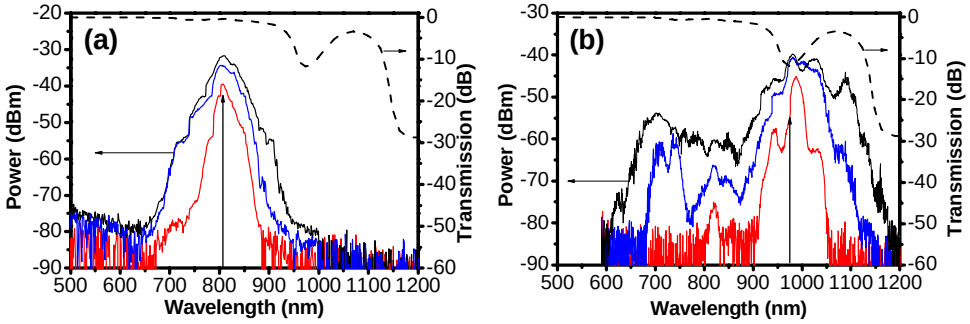

Fig. 2. PCF output spectra with 800-nm (a) and 980-nm (b) pumping for launched peak powers of 90 kW (red) 470 kW (blue) and 940 kW (black). Vertical arrows indicate the pump wavelengths; dashed curves: transmission spectrum over 5 cm of water [19].

The comparison between 800-nm and 980-nm pumping confirms that, as in solid-core PCF supercontinuum generation [5], pumping near the zero-dispersion wavelength (ZDW) is crucial to obtaining a large spectral broadening. In the water-core PCF it is remarkable that the low dispersion at 980-nm by far compensates for the 25-fold increase in attenuation coefficient relative to 800 nm, yielding a spectrum that is 3 times broader at that wavelength. Some insight on the initial dynamics of the spectral broadening at both wavelengths can be gained through a quantitative comparison of the parameters that evaluate the relative importance of nonlinearity, dispersion and attenuation during pulse propagation, namely: the nonlinear length (L_{NL}), the dispersion length (L_D) and the effective length (L_{eff}), respectively [20]. The values for these parameters are the following for 800 nm and 980 nm, respectively: L_{NL}: 7.30×10^{-2} cm and 6.00×10^{-2} cm; L_D: 41.4 cm and 110 cm; L_{eff}: 4.75 cm and 1.81 cm. The fact that $L_{NL}<<L<<L_D$ (with L being the fiber's physical length) for both wavelengths indicates that, indeed, noticeable spectral broadening is expected before the pulses get excessively long. At 980 nm it is seen that L_{eff} is considerably shorter than L, indicating that the nonlinear dynamics practically ceases after the first third of the PCF. The higher dispersion at 800 nm yields a value for L_D that is 2.6 times shorter than that for 980 nm. However, as a drastic spectral broadening takes place, these parameters are only valid for the initial dynamics, explaining the much narrower spectrum for 800 nm pumping. Note that one could be tempted to explain, as in solid-core PCFs, the spectra of Figs. 2(a) and 2(b) as a result of instantaneous self-phase modulation and of soliton formation followed Raman-induced self-frequency shift, respectively. However, the Raman shift in water is much higher (~3000 cm^{-1}) than that of silica (440 cm^{-1}) and the optical Kerr nonlinearity exhibits a 0.7-ps exponential decay [21], affecting the analogy with the dynamics in solid-core PCFs. For a detailed investigation of the supercontinuum dynamics a numerical simulation is under way.

Figure 3 shows a comparison between the continuum generated in the PCF and in the bulk setup with identical launched powers, and both for 800-nm and 980-nm pumping. Figure 3(a) shows the results for 800-nm pumping and 0.94-MW launched peak power. The output spectral width (at -20 dB) is 75 nm in bulk, which is approximately half the width obtained with the PCF (140 nm) and marginally larger than the spectral width of the input pulses. The

#95587 - $15.00 USD Received 29 Apr 2008; revised 7 Jun 2008; accepted 7 Jun 2008; published 16 Jun 2008

results for 980-nm pumping and 1.45-MW launched peak power are depicted in Fig. 3(b). In this case the widths with the bulk and PCF setups are 120 nm and 500 nm respectively (i.e. an over 4× broader spectrum with the PCF). The latter is the broadest width achieved in this work. A further increase in input power led to water evaporation, which can be avoided if both fiber tips are attached to water-filled cuvettes.

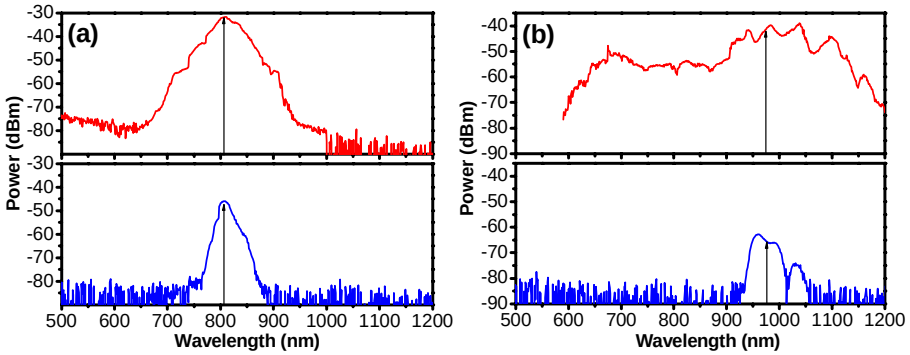

Fig. 3. PCF output spectra with 800-nm and 0.94-MW launched peak power pumping (a) and with 980-nm and 1.45-MW launched peak power pumping (b) for water-core PCF (top) and bulk water (bottom) samples.

Table 1. Summary of the spectral widths (at -20 dB) obtained in water with the tested pump wavelengths and configurations, for a 0.94 MW peak power (except for *: 1.45 MW peak power).

Wavelength (nm)	Bulk	PCF
800	75 nm	140 nm
980	120 nm*	460 nm (500 nm*)

It is evident from Fig. 3 that the spectral broadening is significantly larger in the PCF, which can be attributed to the confinement provided by the waveguide. In the PCF, light is confined to an area comparable to that of the core (~80 μm^2) over the whole ~5-cm length. In contrast, in the bulk setup the beam area at focus can be estimated to be ~800 μm^2 (at ~1 µm and assuming a $1/e^2$ collimated beam diameter of 4 mm), which is kept nearly constant only over a length compared to the confocal parameter (~1.6 mm). These two parameters cannot be simultaneously minimized, which means that changing the focusing lens will not result in a considerable improvement of these values. Note that self-focusing can be neglected at the used power levels. If we define a L_{NL} parameter for the bulk setup using the beam area at focus, its value is 6 mm, which is larger than the confocal parameter and indicates that little spectral broadening is, indeed, expected. Significant (at least a few percent) energy transfer from the pump to the continuum in bulk water usually requires peak powers of hundreds of megawatts or even a few gigawatts (with ~100-fs pulses) [22].

At this point, it is worth pointing out that, although grouped under the common name of supercontinuum generation, the origins of the drastic spectral broadening are significantly different in bulk and waveguide setups. Several authors contributed to the understanding of the supercontinuum dynamics in bulk [23-25] and fiber [5] samples pumped with femtosecond lasers. In bulk, it is well accepted that the continuum results from self-phase modulation resulting from an optical shock wave created by space-time focusing and self-steepening [24]. Chromatic dispersion is show to increase the threshold for self-focusing and, thus, for continuum generation [24,25]. In contrast, waveguide continuum generation (including that reported here) employs much lower powers, for which self-focusing is negligible. In this case, self-phase modulation, stimulated Raman scattering and chromatic dispersion are the main generation mechanisms [5]. To the best of our knowledge, this is the

#95587 - $15.00 USD Received 29 Apr 2008; revised 7 Jun 2008; accepted 7 Jun 2008; published 16 Jun 2008

first time that supercontinuum generation in water is reported in the latter regime and that water's dispersion is exploited to maximize spectral broadening.

The comparison between the spectral widths obtained here with the two pump wavelengths and with bulk and PCF setups is summarized in Table 1. It is apparent that both near-ZDW pumping and waveguide confinement are crucial for supercontinuum generation.

4. Water-core PCF dispersion tuning

The experimental results presented in the previous section show the importance of pumping near the ZDW to achieve the widest spectrum. In this context and to examine the possibility of shifting this wavelength via the fundamental-mode waveguide dispersion of practical PCF designs, we theoretically evaluated the net chromatic dispersion of a number of commercially available hollow-core PCFs [26], the cores of which are filled with water. All PCFs studied were designed for photonic bandgap guidance and have nominal air-filling fractions of >90%. The method described in [27] was used for the evaluation and water's refractive index dependence on wavelength is modeled through equation 12 of [18]. The obtained ZDWs are plotted in Fig. 4 as a function of the core diameter. The monotonic ZDW increase suggests that the core diameter is, indeed, the dominant waveguide dispersion parameter. It is seen that with readily-available PCFs it is possible to tune the ZDW down to 885 nm, meaning that Ti:Sapphire pumping is viable and that the ZDW can be placed at a region of lower attenuation. Note that the fiber used in the experiments could not reliably be modeled, as the observed cladding hole deformations are not compatible with the used method. Nevertheless, Fig. 4 shows that the ZWD is ~1 μm for the commercial 10-μm core diameter PCF.

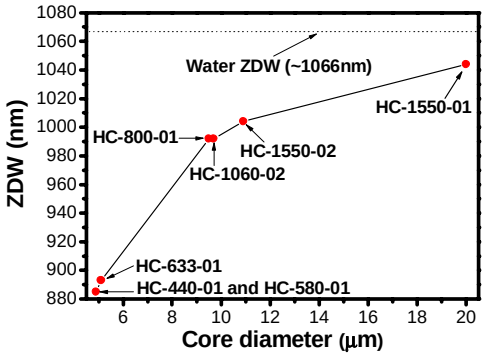

Fig. 4. ZDW as a function of core diameter for commercial PCFs [26] with water-filled cores.

5. Conclusion

Supercontinuum generation was obtained for the first time in a water-core PCF, allowing for the study of this important phenomenon in a regime that was previously unavailable for water. The material dispersion of the liquid was exploited to maximize the spectral broadening. At a maximum input peak power of 1.45 MW the spectrum stretched from ~600 to ~1140 nm, being limited by water's attenuation spectrum. Due to both the high light confinement over a long length and water's low dispersion at the pump wavelength (~980 nm), the supercontinuum generated in the PCF was ~4 times broader than that obtained in a typical bulk setup pumped at same wavelength and power and utilizing a ~7-cm cell. Pumping near the zero-dispersion wavelength was shown to be crucial and an 800-nm pump resulted in a spectral width of only ~140 nm. Zero-dispersion tuning in water-core PCFs was theoretically demonstrated via selection of appropriate commercially available hollow-core PCFs.

Acknowledgments

This work was supported by CAPES (PROCAD grant no. 0156/05-1), Fundo Mackenzie de Pesquisa (MACKPESQUISA), FAPESP and CNPq.

#95587 - $15.00 USD Received 29 Apr 2008; revised 7 Jun 2008; accepted 7 Jun 2008; published 16 Jun 2008